

Activation of Guanosine 5'-[γ - 35 S]thio-triphosphate Binding through M₁ Muscarinic Receptors in Transfected Chinese Hamster Ovary Cell Membranes: 1. Mathematical Analysis of Catalytic G Protein Activation

MAGALI WAELBROECK

Department of Biochemistry and Nutrition, Medical School, Université Libre de Bruxelles, Brussels, Belgium

Received August 8, 2000; accepted January 9, 2001

This paper is available online at <http://molpharm.aspetjournals.org>

ABSTRACT

I analyzed in this work the effect of agonists and unlabeled guanyl nucleotides on [35 S]GTP γ S and [3 H]NMS binding to transfected CHO cells expressing hM₁ muscarinic receptors. I was unable to explain my kinetic results by "traditional" (one-site, two-site, or two-step) bimolecular binding models. I therefore examined the equations that describe catalytic G protein activation. My results were fully consistent with the following interpretation: G protein-coupled receptors either interacted with GDP-bound G proteins and facilitated the GDP release or recognized empty G proteins, depending on the incubation

conditions. The receptor-coupled empty G proteins (RG) then recognized GTP γ S, and the occupied G protein (G $_{GTP\gamma S}^*$) dissociated reversibly from the receptor. Agonists accelerated the GDP release from receptor-coupled G proteins and accelerated the G $_{GTP\gamma S}^*$ dissociation: both effects accelerated synergically the G protein-GTP γ S association reaction in the presence of GDP. GTP γ S-bound G proteins, G $_{GTP\gamma S}^*$, competed efficiently with inactive (empty or GDP-bound) G proteins for receptor recognition, and were able, therefore, at low concentrations, to quench the [35 S]GTP γ S binding reaction.

To further the understanding of biochemical and pharmacological systems, it is essential to translate molecular models (A recognizes B then. . .) into a mathematical description of the system's properties, then confront the equations' predictions with experimental observations. As discussed below, mathematical models describing agonists and antagonists binding to G protein-coupled receptors (GPCRs) have been developed and validated. In contrast, mathematical models describing the effect of agonists on the G protein-guanyl nucleotide interaction are scarce and have rarely been confronted with experimental observations.

Muscarinic receptors belong to the G protein-coupled receptor superfamily. The ternary complex model (De Lean et al., 1980) assumes that agonists (H) stabilize a ternary complex, HRG, involving the receptor (R) and its cognate empty G protein (G). The equations describing this model predict

that agonists discriminate two binding states with high (HRG) and low (HR) affinities provided that 1) they increase the G protein's affinity for the receptor, 2) the resultant interaction is sufficient to induce significant HRG accumulation, and 3) the G protein density is lower than the receptor density. Like β -adrenergic agonists (De Lean et al., 1980), muscarinic agonists probably stabilize ternary complexes with their cognate G proteins: they discriminate high- and low-affinity receptors in the absence of guanyl nucleotides (Birdsall et al., 1978; Hulme et al., 1981; Waelbroeck et al., 1982), and solubilized receptors associate with G proteins in the presence of agonists (Florio and Sternweis, 1985; Haga et al., 1985, 1986). Guanyl nucleotides decrease the G protein's affinity for muscarinic receptors: the "high-affinity" receptor density is markedly decreased or abolished in the presence of guanyl nucleotides (Hulme et al., 1981; Waelbroeck et al., 1982), and guanyl nucleotides destabilize the receptor-G protein interaction (Berrie et al., 1984; Florio and Sternweis, 1985; Haga et al., 1985, 1986).

G proteins hydrolyze GTP to GDP and inorganic phosphate, then release the phosphate ion. GDP is trapped inside the resting G protein in a binding pocket that is stabilized by the α -G β γ interaction: it cooperates with the G β γ subunit

Supported by Grant 3.4504.99 from the Fonds de la Recherche Scientifique Médicale, by an "Action de Recherche Concertée" from the "Communauté Française de Belgique" and by a "Interuniversity Poles of Attraction Program - Belgian State, Prime Minister's Office - Federal Office for Scientific, Technical and Cultural Affairs".

¹ Because of the length of the Appendix, it is not printed herein. It can be found in its entirety in the online version of this article.

ABBREVIATIONS: GPCR, G protein-coupled receptors; GTP γ S, guanosine 5'-thio-triphosphate; CHO, Chinese hamster ovary cells; 4-DAMP mustard, [4-diphenylacetoxy-1-(2-chloroethyl) piperidine]; [3 H]NMS, *l*-[N-methyl- 3 H]scopolamine methyl chloride; DMEM, Dulbecco's minimum essential medium; G $_{GTP}^*$, GTP-bound G proteins; G $_{GTP\gamma S}^*$, GTP γ S-bound G proteins.

in maintaining the $G\alpha$ subunit in its inactive conformation. GTP recognition is necessary to activate the $G\alpha$ subunit, decrease its affinity for $G\beta\gamma$, and facilitate their dissociation. The two isolated G protein subunits may then interact with their messengers (enzyme or channel) (Birnbaumer and Birnbaumer, 1995; Hamm, 1998).

Two interpretations of the role of GPCRs in G protein activation can be found in the literature. Some researchers assumed that agonist-bound receptors favor GTP over GDP binding to the G protein at equilibrium (Costa et al., 1992; Onaran et al., 1993); others assumed that they catalyze the GDP/GTP exchange reaction on their cognate G proteins (Cassel and Selinger, 1978; Mackay, 1990; Krumins et al., 1997; Mukhopadhyay and Ross, 1999). The distinction between these two model families is significant from thermodynamic and molecular points of view. G proteins "know" about agonist binding only during their association with GPCRs: agonists can affect the G protein-GDP/GTP affinities only if stable quaternary HRG-nucleotide complexes accumulate. To increase GTP over GDP binding allosterically at equilibrium, agonists should stabilize the RG_{GTP}^* , RG_{GTP} , or $RG\beta\gamma$ complexes; destabilize the RG_{GDP} complex; or both (Onaran et al., 1993). In contrast to allosteric effectors, catalysts take advantage of transient interactions with the reactants to accelerate the forward and reverse reactions, without affecting the reaction's equilibrium constant. If a high free-energy barrier prevents the GDP/GTP exchange reaction, agonist-bound receptors that decrease this barrier can accelerate GTP (or GDP) binding to several G proteins in turn (Waelbroeck, 1999).

I expected to easily discriminate these two models by analyzing the effect of muscarinic agonists on guanyl nucleotides binding to transfected CHO cells. [^{35}S]GTP γ S binding and dissociation were slow: I therefore attempted to evaluate the G protein binding properties using nonequilibrium GTP γ S binding models. The [^{35}S]GTP γ S binding kinetics could not be explained by "traditional" (one-site, two-site, or two-step) bimolecular binding models: a catalytic model of G protein activation was necessary to understand the [^{35}S]GTP γ S binding kinetics of CHO cell G proteins.

Experimental Procedures

Materials. Stably transfected CHO cells expressing the human M_1 muscarinic receptor subtype (Hm1 CHO cells) were a generous gift from Dr. N. Buckley (London, England). 4-Diphenylacetoxy-1-(2-chloroethyl) piperidine (4-DAMP) mustard was a generous gift from Dr. R. Barlow (Kirkby Stephen, Cumbria, UK). *L*-[N -methyl- ^3H]scopolamine methyl chloride ([^3H]NMS; 80 Ci/mmol) and guanosine 5'-[γ - ^{35}S]thio-triphosphate, triethylamine salt ([^{35}S]GTP γ S; >1000 Ci/mmol) were obtained from Amersham Pharmacia Biotech (Bucks, UK). Unlabeled guanyl nucleotides (as Li^+ salts) were obtained from Roche Molecular Biochemicals (Mannheim, Germany). Acetylcholine chloride and pertussis toxin were obtained from Sigma Chemical Co (St. Louis, MO), and carbamylcholine hydrochloride from Merck (Darmstadt, Germany). The cell culture media were obtained from Life Technologies (Gent, Belgium). All other chemicals were of the highest grade available.

Methods

Cell culture and harvesting. The Hm1 CHO cells stock culture was maintained in Dulbecco's minimal essential medium, enriched with 10% fetal calf serum, 200 $\mu\text{g}/\text{ml}$ geneticin, 2 mM glutamine, 100 IU/ml penicillin, and 100 $\mu\text{g}/\text{ml}$ streptomycin. Geneticin was not

included in subcultures prepared for binding and functional assays. Barely confluent (control or pretreated) CHO cells were harvested in a 20 mM HEPES/NaOH buffer enriched with 10 mM EDTA, pH 7.4, and homogenized in a glass/Teflon homogenizer before centrifugation at 20,000g for 20 min. The pellet was resuspended in a 20 mM HEPES/NaOH buffer enriched with 0.1 mM EDTA, pH 7.4, and recentrifuged at 20,000g for 20 min. The pellet was resuspended in the binding buffer (see below), frozen in liquid nitrogen, and stored at -80°C until use. [Cell culture and harvesting adapted from Lazareno et al. (1993).]

[^{35}S]GTP γ S and [^3H]NMS Binding to Membranes. Binding of both tracers was studied at 30°C in 1 ml of 20 mM HEPES/NaOH buffer enriched with 100 mM NaCl and 5 mM MgCl_2 , pH 7.4, in the absence or presence of the indicated agonist and/or guanyl nucleotide concentrations (Lazareno et al., 1993). The tracer concentrations were either 800 pM [^3H]NMS or 50 pM [^{35}S]GTP γ S. Unless otherwise indicated, the incubation period was 10 min at 30°C in the absence of unlabeled nucleotide, or 1 h at 30°C when 3 μM GDP or 1 μM GTP was included in the binding buffer. The membrane concentration (0.1 to 0.2 mg of protein per milliliter) was adjusted to achieve 10 to 20% of tracer binding under these incubation conditions.

Nonspecific [^3H]NMS and [^{35}S]GTP γ S binding was defined as tracer binding in the presence of 10 μM atropine or 100 μM GTP, respectively, and was subtracted from total binding measurements. It reflected in both cases tracer binding to the filters, and represented 0.3 to 1% of the radioactivity offered.

Tracer binding was determined by liquid scintillation counting, after filtration through glass-fiber filters (Gelman A/C; Gelman Sciences, Ann Harbor, MI). The composition of the buffer used to rinse the filters did not seem to affect the results: we therefore rinsed them three times with ice-cold 50 mM sodium phosphate buffer, pH 7.4, for [^3H]NMS as well as [^{35}S]GTP γ S binding studies.

Pretreatment with 4-DAMP Mustard. A 4-DAMP mustard stock solution (10 mM) was prepared in 0.1 N acetic acid and stored at -20°C until use (within 1 month). This solution was diluted to 3, 10 or 30 μM in a 10 mM sodium phosphate buffer, pH 7.4, then further diluted 1000-fold in DMEM (to 3, 10, or 30 nM). Confluent cells were rinsed twice with DMEM to remove the fetal calf serum before treatment with the 4-DAMP mustard/DMEM solution. After 1 h incubation at 37°C , the medium was aspirated and the cells were rinsed twice with fresh DMEM before use.

Data Analysis. Nonlinear curve fitting of the dose-effect and competition curves was performed with a computer assisted curve fitting program (Prism; GraphPAD Software, San Diego, CA). The agonists K_H , K_L , and corrected IC_{50} values were calculated by the Cheng-Prusoff equation (1973). The GTP γ S association kinetics were analyzed with the help of a spreadsheet, as described previously (Waelbroeck et al., 1989).

Results

Preliminary Assays. To evaluate the stability of the G proteins in my incubation conditions, I delayed tracer addition for up to 2 h at 30°C before measuring [^{35}S]GTP γ S binding after a short (10 min) incubation. If the membranes were preincubated for 1 h or more at 30°C before tracer addition, the subsequent tracer binding decreased slowly with increasing preincubation periods (not shown). This suggested that, as previously described for solubilized G proteins (Chidiac et al., 1999), the G proteins were not stable over several hours at this temperature. I therefore cannot guarantee that equilibrium was really achieved after 1 h incubation: the [^{35}S]GTP γ S binding plateau observed between 60 and 120 min of incubation perhaps represented continued [^{35}S]GTP γ S binding balanced by $G_{GTP\gamma S}^*$ denaturation.

Presence of GDP-Bound G Proteins? The [^{35}S]GTP γ S association rate is, by definition, proportional to the reac-

tants' concentrations ([³⁵S]GTP γ S and empty G proteins) and to their association rate constant. On theoretical grounds, agonists may accelerate GTP γ S binding by increasing the empty G protein concentration, their association rate constant (k_{on}), or both. Because there is only one guanyl nucleotide binding site per G protein, GDP-bound G proteins cannot recognize GTP γ S. The GDP release from purified G proteins is so slow that it can become rate limiting, leading to anomalous [³⁵S]GTP γ S binding kinetics (very low apparent k_{on} value, association rate independent of the GTP γ S concentration) (Ferguson et al., 1986). Muscarinic agonists, which markedly accelerate the GDP dissociation, are able to increase the available (empty) G protein concentration and facilitate GTP γ S recognition (Berstein et al., 1992).

In contrast with the results of Ferguson et al. (1986), the GTP γ S association rate was large [$k_{on} \approx 10^6$ - 10^8 M⁻¹min⁻¹ compared with 6×10^4 M⁻¹min⁻¹ (Ferguson et al., 1986)], and proportional to the tracer concentration (see Fig. 1). This

result suggested that most of the membrane-bound G proteins might be readily available for GTP γ S recognition in my assay. To verify this hypothesis, I measured [³⁵S]GTP γ S binding to membranes preincubated with or without an agonist, as explained below.

If the membrane preparation procedure was too short to allow significant GDP release, merely preincubating the membranes in the presence of agonists and in the absence of GDP should be sufficient to increase the empty G protein concentration available for subsequent GTP γ S recognition and thereby accelerate [³⁵S]GTP γ S binding. On the other hand, if all G proteins had sufficient time to release GDP during the membrane preparation, the continued presence of agonists that increase the GTP γ S association rate constant would be necessary to accelerate [³⁵S]GTP γ S recognition.

I tested these hypotheses; my findings are reported in Table 1. Carbamylcholine-receptor complexes increased [³⁵S]GTP γ S binding (compare rows 2 and 3 with row 1). In contrast, merely preincubating the membranes with an agonist was not sufficient to facilitate [³⁵S]GTP γ S binding (row 4). My results suggested that the accessible G proteins in my membrane preparation were already empty and that agonist-bound receptors increased the GTP γ S association rate constant by affecting the binding properties of "empty" G proteins.

[³⁵S]GTP γ S Binding Kinetics Analysis. The [³⁵S]GTP γ S association rate was monoexponential (Fig. 1). In contrast, its dissociation rate was markedly biphasic (Fig. 1), suggesting that different [³⁵S]GTP γ S-bound G protein subtypes or states ($G_{GTP\gamma S}^*$ and $RG_{GTP\gamma S}^*$) coexisted in this membrane preparation.

Bimolecular association models predict that the rate at which equilibrium is reestablished is independent of the starting point if the tracer or G protein concentrations are vanishingly low. This is because both concentrations appear only simultaneously, as $k_{on}[GTP\gamma S][G]$ products in the rate equation $v = d[G_{GTP\gamma S}] / d(t)$. In results at very low GTP γ S concentrations, the dissociation kinetic should be symmetrical with the association kinetic (Fig. 2, top and center). If the tracer recognizes a single binding site (model 1, $G + GTP\gamma S \leftrightarrow G_{GTP\gamma S}^*$), the association and dissociation kinetics should be monoexponential, and the pseudo first-order association rate constant I obtained (using a very low [³⁵S]GTP γ S concentration) should be equivalent to the [³⁵S]GTP γ S dissociation rate constant (Fig. 2, top). The [³⁵S]GTP γ S dissociation rate was biphasic (Fig. 1, bottom), suggesting that the tracer

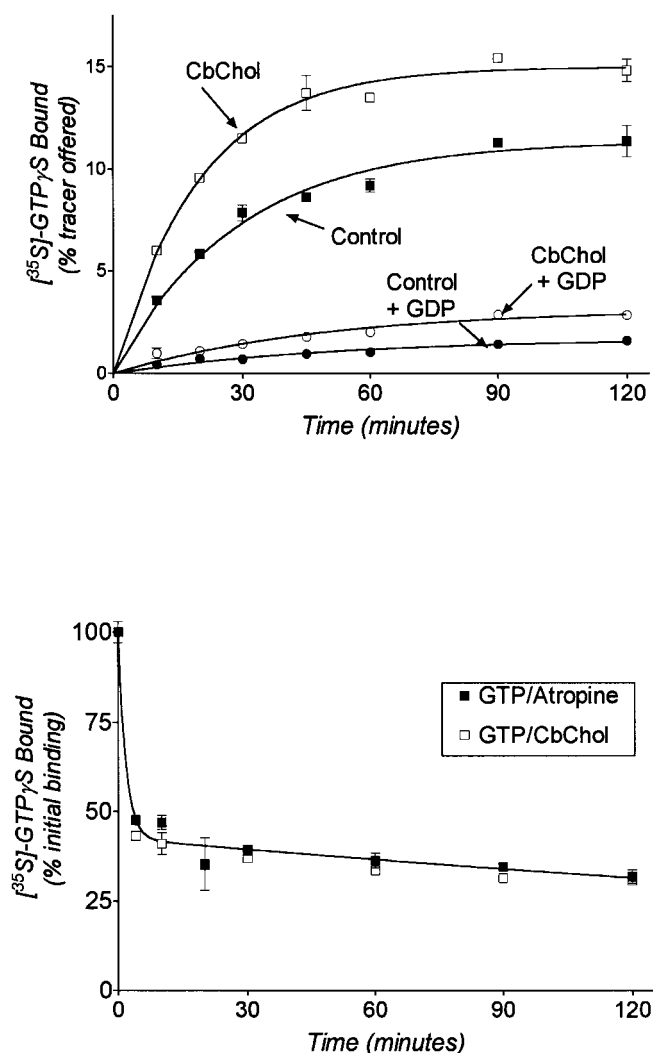


Fig. 1. [³⁵S]GTP γ S binding kinetics. Top, [³⁵S]GTP γ S binding to CHO cell membranes was measured after the indicated incubation periods, in the absence (closed symbols) or presence (open symbols) of 1 mM carbamylcholine and in the absence (squares) or presence (circles) of 3 μ M GDP. The results are expressed as average \pm SEM of triplicate determinations. Representative of at least two duplicate experiments. Bottom, [³⁵S]GTP γ S dissociation was induced after 10 min preincubation by addition of a large excess (100 μ M) of GDP in the absence or presence of carbamylcholine. Representative of three experiments in duplicate.

TABLE 1

[³⁵S]GTP γ S binding to CHO cell membranes that were preincubated 10 min in the absence or presence of agonists

Four sets of membrane samples were preincubated for 10 min in the absence or presence of 1 mM carbamylcholine. [³⁵S]GTP γ S binding (\pm SEM) was measured after a second 10-min incubation in the absence or presence of carbamylcholine or after addition of 10 μ M atropine, as indicated. The results are expressed as percentage of [³⁵S]GTP γ S binding in the absence of carbamylcholine. (Representative of two duplicate experiments.)

Preincubation	Incubation	[³⁵ S]GTP γ S binding %
Buffer	Buffer	100 \pm 6
Buffer	+ Carbamylcholine (1 mM)	139 \pm 7
Carbamylcholine (1 mM)	Carbamylcholine (1 mM)	128 \pm 8
Carbamylcholine (1 mM)	+ Atropine (10 μ M)	97 \pm 3

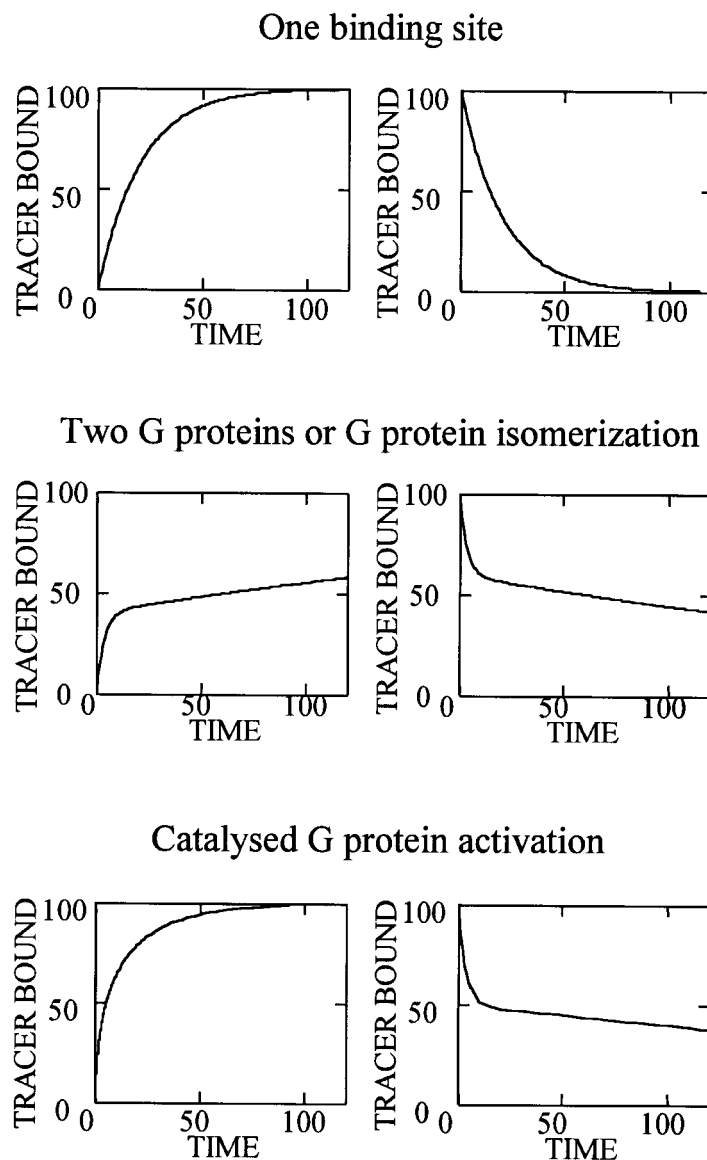


Fig. 2. Comparison of the nucleotide binding and dissociation kinetic patterns that might be expected from the following reaction mechanisms: $G + GTP\gamma S \leftrightarrow G_{GTP\gamma S}^*$ (top); $G + GTP\gamma S \leftrightarrow G_{GTP\gamma S} \leftrightarrow G_{GTP\gamma S}^*$ or $G1 + G2 + GTP\gamma S \leftrightarrow G1_{GTP\gamma S} + G2_{GTP\gamma S}$ (center); $G + GTP\gamma S + \{R \leftrightarrow RG + GTP\gamma S \leftrightarrow RG_{GTP\gamma S} \leftrightarrow R\} + G + G_{GTP\gamma S}^*$ (bottom). (Tracer binding is expressed as percentage of equilibrium.) I assumed in the three left panels that the tracer was present at a vanishingly low concentration ($[^{35}S]GTP\gamma S/K_D \approx 0$) and expressed all binding data as percentage of the equilibrium binding. The top panels represent the association and dissociation kinetics expected if all binding sites had the same rate constant $k_{off} = 0.05 \text{ min}^{-1}$. In the center panels, I assumed either that the two binding sites or states release $[^{35}S]GTP\gamma S$ with (apparent) dissociation rate constants $k_{off}^1 = 0.3 \text{ min}^{-1}$ and $k_{off}^2 = 0.003 \text{ min}^{-1}$. The bottom panels represent the $[^{35}S]GTP\gamma S$ binding and dissociation kinetics under the assumption that the empty G protein concentration was large during the association kinetics ($[G_e] / K_m^G = 2$), became saturating upon GTP γS binding ($[G_{GTP\gamma S}^*] / K_m^{GTP\gamma S} = 100$) and negligible after GDP recognition ($[G_{GDP}] / K_m^{GDP} \approx 0$) and that the maximal forward and reverse rates were $V_{max}^f = 200 \text{ min}^{-1}$ and $V_{max}^r = 0.2 \text{ min}^{-1}$, respectively. I assumed in addition that the receptor concentration was so large that the $R_{GTP\gamma S}^*$ concentration (Equation A.6; see Appendix) represented 50% of the tracer binding at the dissociation onset. The subscripts "0", "t," and "e" in the following equations indicate that the (free or occupied) G protein concentration is taken at time 0, at the given time point, and at equilibrium, respectively. The receptor-catalyzed $[^{35}S]GTP\gamma S$ association (in the absence of GDP) and dissociation (in the presence of GDP) kinetics is described by the equations

$$time = \left(1 + \frac{[G_{GTP\gamma S}]_e}{K_m^{GTP\gamma S}} \right) \frac{[G_{GTP\gamma S}]_e}{K_m^{GTP\gamma S}} \ln \left(\frac{[G_{GTP\gamma S}]_e}{[G_{GTP\gamma S}]_t - [G_{GTP\gamma S}]_e} \right) - \frac{[G_{GTP\gamma S}]_e}{V_{max}^f} \frac{[G_{GTP\gamma S}]_t}{K_m^{GTP\gamma S}} \frac{[G_e]_0}{K_m^{G_e}} \quad (1)$$

and,

$$time = \left(1 + \frac{[G_{GDP}]_0}{K_m^{GDP}} \right) \ln \left(\frac{[G_{GTP\gamma S}]_0}{[G_{GTP\gamma S}]_t} \right) + \frac{1}{V_{max}^r} \left(1 + \frac{[G_{GDP}]_0}{K_m^{GDP}} \frac{V_{max}^r}{[G_{GTP\gamma S}]_0} \right) \left(\frac{[G_{GTP\gamma S}]_0}{K_m^{GTP\gamma S}} - \frac{[G_{GTP\gamma S}]_t}{K_m^{GTP\gamma S}} \right) \quad (2)$$

respectively. [Equations developed by analogy to eq. 2.58 on page 46 of Cornish-Bowden (1995)].

recognized two different G proteins, or that two occupied G protein states coexisted upon tracer binding: $G1 + G2 + \text{GTP}\gamma\text{S} \leftrightarrow G1^*_{\text{GTP}\gamma\text{S}} + G2^*_{\text{GTP}\gamma\text{S}}$ or: $G + \text{GTP}\gamma\text{S} \leftrightarrow G_{\text{GTP}\gamma\text{S}} \leftrightarrow G^*_{\text{GTP}\gamma\text{S}}$. The tracer association rate, measured at a very low tracer concentration (Fig. 2 center), should also be biphasic in these cases. It was thus impossible to simultaneously fit the GTPγS association and dissociation kinetics using bimolecular (G protein/GTPγS) binding models.

As discussed in the appendix,¹ if the GTPγS-G protein recognition and dissociation reactions are catalyzed by GPCRs, GTPγS-bound G proteins might compete with empty G proteins for receptor recognition during the association phase and empty or occupied (unlabeled nucleotide-bound) G proteins with GTPγS-bound G proteins during the dissociation phase. There, results that the rate at which equilibrium is reached in association and dissociation kinetics depends on the G protein status (concentrations of empty, GDP-bound, GTPγS bound G proteins?). I did not attempt to fit my data to the catalytic model equations (they involve too many parameters), but I did verify that kinetics similar to my experimental data can be predicted by the catalytic model of G protein activation (Fig. 2, bottom).

Effect of Agonists on [³⁵S]GTPγS Binding. Acetylcholine or carbamylcholine, acting through M₁ muscarinic receptors, accelerated the [³⁵S]GTPγS recognition in the absence as well as in the presence of added GDP or GTP (Fig. 1, top, and results not shown). (This is a rather unusual result: GDP addition to the incubation medium is usually essential to observe increased [³⁵S]GTPγS binding in response to agonists). Agonists increased tracer binding to slowly- and rapidly-dissociating [³⁵S]GTPγS binding sites to the same extent (not shown): G proteins from both populations were coupled to M₁ muscarinic receptors. Muscarinic agonists, such as the muscarinic antagonist atropine nevertheless did not detectably affect the [³⁵S]GTPγS dissociation rate constants or the proportion of rapidly/slowly dissociating $G^*_{\text{GTP}\gamma\text{S}}$ complexes (Fig. 1, bottom). [Again, this is unusual: agonists activating $G_{i/o}$ proteins through membrane-bound cardiac muscarinic M₂ (Hilf and Jakobs, 1992), fMet-Leu-Phe (Kupprion et al., 1993), or opiate (Breivogel et al., 1998) receptors either increased the proportion of rapidly dissociating $G^*_{\text{GTP}\gamma\text{S}}$ complexes or accelerated the [³⁵S]GTPγS dissociation rate.] These results suggested that muscarinic M₁ agonists increased the GTPγS affinity for receptor-coupled G proteins, increased the available G protein density, or both. I performed homologous [³⁵S]GTPγS/GTPγS competition curves to study this problem.

GTPγS Competition Curves and G Protein Density Evaluation. [³⁵S]GTPγS/GTPγS competition curves were monophasic ($n_H \approx 1$) in the absence of agonist. They shifted to significantly lower concentrations with increasing incubation periods (Fig. 3), as expected for a ligand that dissociates very slowly from its binding sites (Motulsky and Mahan, 1984). The GTPγS association kinetics and nonequilibrium competition curves could be fitted by a bimolecular association model using the following parameters: k_{on} , $7 \times 10^6 \text{ M}^{-1}\text{min}^{-1}$; k_{off} , $2.3 \times 10^{-2} \text{ min}^{-1}$; and B_{max} , 18 pmol/mg protein (Motulsky and Mahan, 1984). The dissociation rate constant extracted from Fig. 3, however, was not compatible with either the rapid (k_{off} , $0.55 \pm 0.15 \text{ min}^{-1}$) or slow (k_{off} , $2.5 \pm 0.8 \times 10^{-3} \text{ min}^{-1}$) dissociation phases observed in Fig. 1.

Irreversible bimolecular reactions, reversible bimolecular

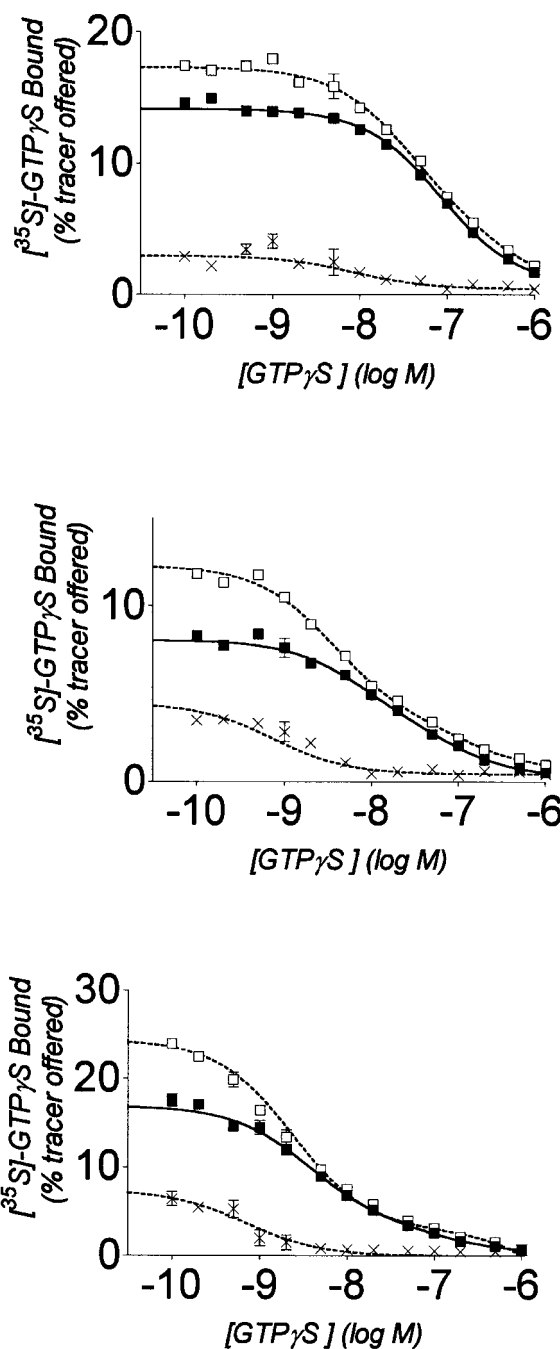


Fig. 3. Effect of the incubation period on [³⁵S]GTPγS/GTPγS competition curves. Homologous [³⁵S]GTPγS/GTPγS competition curves were obtained after incubations of 2 min (top), 10 min (center), or 1 h (bottom panel), in the absence (■) or presence (□) of 1 mM carbamylcholine. (The membrane concentration was increased 4-fold for the 2-min incubation to compensate for the short incubation period). The apparent GTPγS affinity ($pI_{50} = -\log IC_{50}$ value) increased in the presence of carbamylcholine, from 7.03 ± 0.08 to 7.19 ± 0.06 , from 7.73 ± 0.04 to 8.08 ± 0.08 and from 8.26 ± 0.03 to 8.50 ± 0.04 after 2, 10, and 60 min of incubation, respectively. The control competition curves were compatible with the existence of a single site (n_H , 0.88 ± 0.11 , 1.02 ± 0.08 , and 0.96 ± 0.04 after 2, 10, and 60 min of incubation, respectively). The competition curves obtained in the presence of carbamylcholine were shallow (n_H , 0.70 ± 0.04 , 0.78 ± 0.04 , and 0.73 ± 0.04 after 2, 10, and 60 min of incubation, respectively). "Over-basal": the difference between the two curves at each GTPγS concentration is represented by the "x" symbols. The over-basal competition curves were compatible with agonist-dependent labeling of a single high-affinity GTPγS binding site (n_H , 1.07 ± 0.25 , 0.92 ± 0.09 , and 0.92 ± 0.12 ; pI_{50} values, 8.15 ± 0.28 , 8.87 ± 0.09 , and 9.57 ± 0.10 after 2, 10, and 60 min of incubation, respectively). Representative of at least two duplicate experiments.

reactions, and catalyzed association reactions yield almost superimposable saturation curves at very different binding site densities. If the equilibrium binding model were used to analyze nonequilibrium saturation curves (obtained after incubations that were too short), the binding site concentration would be significantly overestimated, but if an irreversible binding model were used to analyze equilibrium saturation curves, B_{\max} would be underestimated (Motulsky and Mahan, 1984). If the binding reaction is catalyzed, during the very short period in which binding is proportional to the incubation period at all ligand concentrations, the apparent "best-fit B_{\max} " will be proportional to the incubation period, and very much lower than the real total binding sites concentration (Appendix).

The apparent B_{\max} obtained under the (incorrect) assumption that "equilibrium binding has been achieved" decreased with increasing incubation periods. This suggested that the third model is not applicable: the "best-fit B_{\max} " is not proportional to the incubation period. It also suggested that equilibrium was not achieved. The B_{\max} obtained assuming irreversible binding, however, increased: GTP γ S binding was slow but not irreversible. Using an irreversible binding model, the 10-min competition curve was compatible with a B_{\max} value of 13 pmol/mg protein; the same competition curve fitted with an equilibrium binding model yielded a GTP γ S B_{\max} of 20 pmol/mg protein. Therefore, I concluded that the GTP γ S binding sites concentration was at least 13 pmol/mg protein, probably close to the 18 pmol/mg protein found using the "slowly reversible" binding model.

Agonists significantly increased [35 S]GTP γ S binding at low nucleotide concentrations. The [35 S]GTP γ S/GTP γ S competition curves obtained in the presence of agonists were biphasic, suggesting that GTP γ S discriminated two binding site populations in the presence of agonists (Fig. 3). I calculated the "over-basal" (agonist-induced) tracer binding at each GTP γ S concentration and obtained monophasic competition curves. The over-basal GTP γ S association kinetics and non-equilibrium competition curves could be fitted with the following parameters: k_{on} , $1.6 \times 10^8 \text{ M}^{-1} \text{ min}^{-1}$; k_{off} , $3.0 \times 10^{-2} \text{ min}^{-1}$; and B_{\max} , 700 fmol/mg protein. As above, the dissociation rate constant extracted from these data was not compatible with either the fast or slow [35 S]GTP γ S dissociation phase observed in Fig. 1. The over-basal (10 min incubation) GTP γ S competition curve, fitted with an irreversible and an equilibrium binding model, yielded B_{\max} values between 490 and 750 fmol/mg protein (Fig. 4): muscarinic agonists affected only 3 to 6% of the total CHO cell G protein population, or at least 0.5 G proteins per receptor (940 ± 40 fmol/mg protein; see below).

Effect of the Receptor and G Protein Concentrations on the Initial [35 S]GTP γ S Association Rate. If [35 S]GTP γ S recognizes all (uncoupled as well as receptor-coupled) G proteins, its association rate should be proportional to the total G protein concentration. In contrast, if it recognizes RG complexes only, the G protein association rate might be proportional to the receptor rather than G protein concentration (for $[R_{\text{tot}}] < [G_{\text{tot}}]$). To decrease the total G protein concentration, I pretreated CHO cells 16 h before harvesting with 100 ng/ml pertussis toxin. [35 S]GTP γ S binding in the presence of GDP decreased markedly in treated cell membranes, but the initial [35 S]GTP γ S binding rate, measured in the absence of unlabeled guanyl nucleotides, was

unaffected. These results suggested that, in the absence of GDP, CHO cell G proteins interacted with resting GPCRs and that, even in the absence of agonists, [35 S]GTP γ S recognized preferentially receptor-coupled empty G proteins.

To decrease the muscarinic receptor concentration, I pretreated CHO cells with 4-DAMP mustard. I then analyzed homologous [35 S]GTP γ S/GTP γ S competition curves (as above) to evaluate the agonist-regulated G protein population density (Table 2). The over-basal [35 S]GTP γ S binding (measured at a very low tracer concentration) was proportional to the muscarinic receptor concentration: as expected, [35 S]GTP γ S recognized ternary complexes (HRG) in response to agonists.

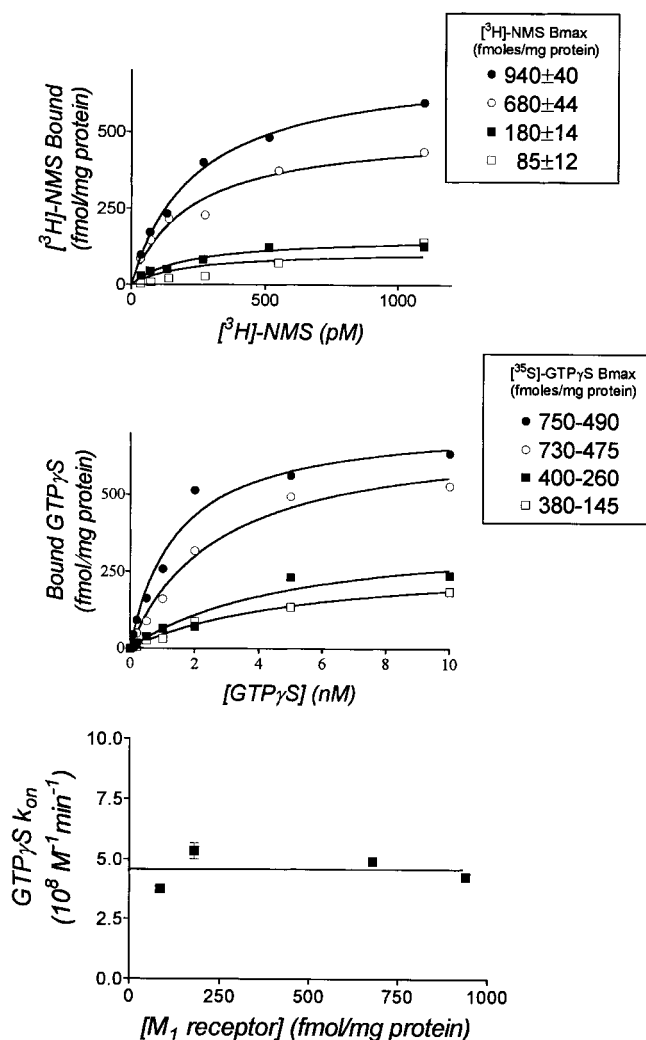


Fig. 4. Effect of 4-DAMP mustard on the [^3H]NMS (top) and on the over-basal [^{35}S]GTP γ S (center) saturation curves. Top, [^3H]NMS saturation curves (B_{\max}) obtained in control membranes (\bullet , 940 ± 40 fmol/mg of protein) and in membranes pretreated with 3 nM (\circ , 680 ± 44 fmol/mg of protein), 10 nM (\blacksquare , 180 ± 14 fmol/mg of protein), or 30 nM (\square , 85 ± 12 fmol/mg of protein) 4-DAMP mustard. Center, [^{35}S]GTP γ S/GTP γ S saturation curves (B_{\max}) obtained in control membranes (\bullet , $750\text{--}490$ fmol/mg of protein) and in membranes pretreated with 3 nM (\circ , $730\text{--}475$ fmol/mg of protein), 10 nM (\blacksquare , $400\text{--}260$ fmol/mg of protein), or 30 nM (\square , $380\text{--}145$ fmol/mg of protein) 4-DAMP mustard. The bound GTP γ S concentration was calculated by multiplying the bound [^{35}S]GTP γ S fraction by the total GTP γ S concentration offered. The [^3H]NMS and [^{35}S]GTP γ S B_{\max} values obtained from this experiment are summarized in Table 3. (Representative of at least three duplicate experiments.) Bottom, initial GTP γ S association rate constants, calculated using the equation $v = [G_{\text{GTP}\gamma\text{S}}] / \text{min} = k_{\text{on}} [R_{\text{tot}}][\text{GTP}\gamma\text{S}]$.

At the lower receptor concentrations studied, each agonist-bound receptor was capable of inducing GTPγS binding to several (2 or more) G proteins (Fig. 4). This result supported the hypothesis that activated (GTPγS-bound) G proteins could be released by agonist-bound receptors, thereby allowing each receptor to facilitate, sequentially, [³⁵S]GTPγS binding to several G proteins.

Agonist Dose Effect Curves on [³⁵S]GTPγS Binding. The muscarinic agonist concentrations necessary to accelerate [³⁵S]GTPγS binding were lower in the absence than in the presence of GDP or GTP (Fig. 5 and Table 3).

If the receptor concentration is too large, activation of a fraction of the available receptors might be sufficient for maximal G protein activation (spare receptors). The agonist EC₅₀ values are then lower than their active site dissociation constants, K_{act} . This hypothesis is easily tested by comparing the dose-effect curves obtained at different receptor densities. In the absence of spare receptors, the agonist E_{max} value is proportional to the receptor density; if the spare receptor proportion is high, E_{max} values are not affected by the receptor density and EC₅₀ decreases with increasing receptor densities. As indicated above, the over-basal [³⁵S]GTPγS binding induced by 1 mM acetylcholine was proportional to the residual M₁ receptor density (Table 2). My results therefore suggested that there were no spare receptors, even in the absence of unlabeled nucleotides ($pEC_{50} = pK_{act}$), and that GDP and GTP decreased significantly the agonists' potency.

Muscarinic Receptor Binding Studies: Comparison of the Agonists' Binding and Functional Properties. [³H]NMS labeled 800 ± 40 fmol/mg protein with a K_D value of 110 ± 20 pM at equilibrium (≥1 h incubation at 30°C). Agonist competition curves in the absence of guanyl nucleotides were compatible with the existence of two muscarinic binding sites or states. Competition curves were obtained at different (0.05 to 5 nM) tracer concentrations after 10-min

and 1-h incubations (not shown), to evaluate the two (high- and low-affinity) K_D values, K_H and K_L (Table 3).

Acetylcholine and carbamylcholine achieved equilibrium binding within 10 min at 30°C. They recognized 31 and 25% of the binding sites (200–240 fmol/mg protein) with a high affinity in the absence of guanyl nucleotides. The acetylcholine and carbamylcholine EC₅₀ values (3.5 and 21 μM, respectively) obtained in the absence of GDP were intermediate between their K_H and K_L values (0.6 and 26 μM for acetylcholine, 1.9 and 224 μM for carbamylcholine, respectively). This result suggested that, at very low guanyl nucleotide concentrations, both receptor states participated to the [³⁵S]GTPγS binding acceleration.

In the presence of micromolar GDP or GTP concentrations, both agonists had homogeneous (low) affinities for M₁ receptors (Table 3), and their EC₅₀ values were identical to their (low affinity) K_D values (30 versus 42 μM, respectively, and 224 versus 588 μM, respectively) (Table 3): high-affinity receptors did not detectably accumulate or participate to the [³⁵S]GTPγS binding reaction under these conditions.

GDP and GTP Competition Curves. GDP and GTP competition curves were shallow in the absence and in the presence of agonists (Fig. 6). They were not affected by pre-incubation with the membranes before [³⁵S]GTPγS addition: both nucleotides were stable in the solution. The GTP and GDP competition curves shifted to slightly higher concentrations after prolonged incubation (1 h) in the presence of [³⁵S]GTPγS, as expected from the increased apparent GTPγS affinity (not shown); both unlabeled nucleotides achieved steady state binding very rapidly.

Acetylcholine and carbamylcholine shifted the competition curves, not only of GDP but also of GTP, to higher concentrations (Fig. 6); muscarinic agonists didn't "favor GTP over GDP binding" under these incubation conditions. The agonist-induced fold stimulation of [³⁵S]GTPγS binding was im-

TABLE 2

Effect of 4-DAMP mustard pretreatment on the muscarinic binding site and acetylcholine induced GTPγS binding site densities. Representative of three experiments.

4-DAMP mustard	[³ H]NMS B_{max}^a fmol / mg of protein	[³ H]NMS B_{max} % of control	Over-basal [³⁵ S]GTPγS B_o^b % control	Over-basal GTPγS pIC ₅₀ Values	Over-basal GTPγS B_{max}^c fmol / mg of protein
Control cells (0)	940 ± 40	100%	100%	8.73 ± 0.16	490–750
3 nM	680 ± 44*	72.3 ± 5%*	75 ± 5%*	8.62 ± 0.17	475–730
10 nM	180 ± 14*	19.2 ± 2%*	19 ± 3%*	8.38 ± 0.26	260–400
30 nM	85 ± 12*	9.0 ± 1.3%*	5 ± 2%*	8.11 ± 0.33	145–380

^a The muscarinic receptor density (B_{max}) was evaluated by non-linear curve fitting of [³H]NMS saturation curves.

^b The difference between "tracer" (50 pM) [³⁵S]GTPγS binding in the absence and presence of acetylcholine (1 mM) was measured after 10 min incubation in the absence of unlabeled nucleotide.

^c These two GTPγS B_{max} value estimates correspond to the values obtained by fitting the over basal GTPγS competition curve with an irreversible and with an equilibrium binding model, respectively (see text). The total GTPγS binding site concentration (measured in the absence of agonist) was between 21 and 32 pmol/mg protein.

*, Significantly different control (0 nM 4-DAMP mustard treatment) ($p < 0.05$).

TABLE 3

Agonist functional and binding properties:

The agonists affinity constants [$pK = -\log(K)$] and potencies [$pEC_{50} = -\log(EC_{50})$] for activation of [³⁵S]GTPγS binding to CHO cell membranes in the absence and presence of GDP were evaluated by nonlinear curve fitting of agonists competition and dose-effect curves. Acetylcholine and carbamylcholine recognized 31 ± 9 and 25 ± 7% of the receptors with a high affinity (K_H) and had a low affinity (K_L) for the remaining sites in the absence of guanyl nucleotides. In the presence of GDP, GTP, or GTPγS, they had a homogeneous low affinity. Average of three to five duplicate experiments.

Agonist	Control			3 μM GDP	
	pK_H	pK_L	pEC_{50}	pEC_{50}	pK_D
Acetylcholine	6.20 ± 0.40	4.58 ± 0.22	5.45 ± 0.19 ^a	4.53 ± 0.15	4.38 ± 0.08
Carbamylcholine	5.72 ± 0.60	3.65 ± 0.13	4.67 ± 0.24 ^a	3.65 ± 0.18	3.23 ± 0.06

^a Significantly different from pK_L .

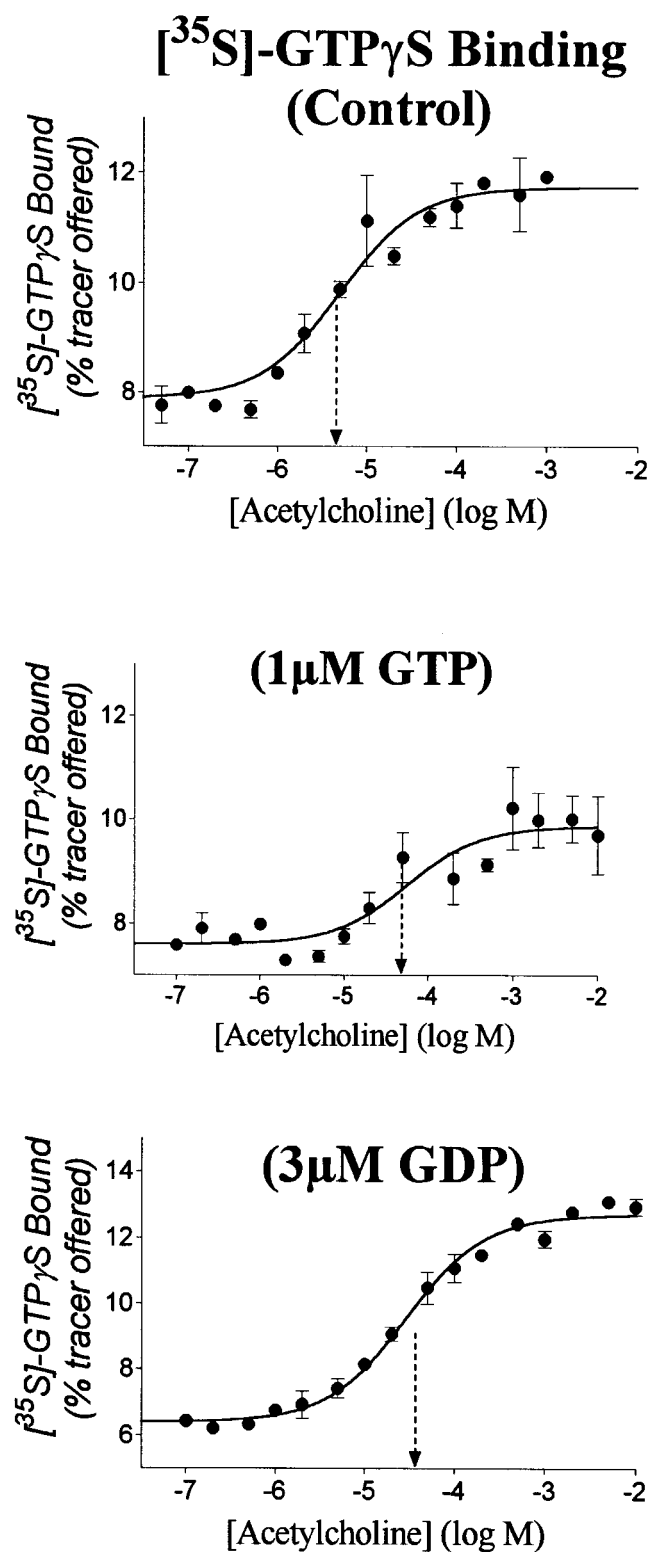


Fig. 5. Agonist dose-effect curves in the absence and presence of GDP or GTP. [³⁵S]GTP_γS binding was measured in the absence or presence of the indicated acetylcholine concentrations, after 10 min incubation in the absence of guanyl nucleotide (top) or after 1 h incubation in the presence of 1 μM GTP (center) or of 3 μM GDP (bottom). The results are represented as percentage ± SEM of "B₀", that is, [³⁵S]GTP_γS binding in the absence of agonist (10% of the added tracer in the absence of unlabeled nucleotide, 7% in the presence of GDP, and 6% in the presence of GTP). Representative of at least three duplicate experiments.

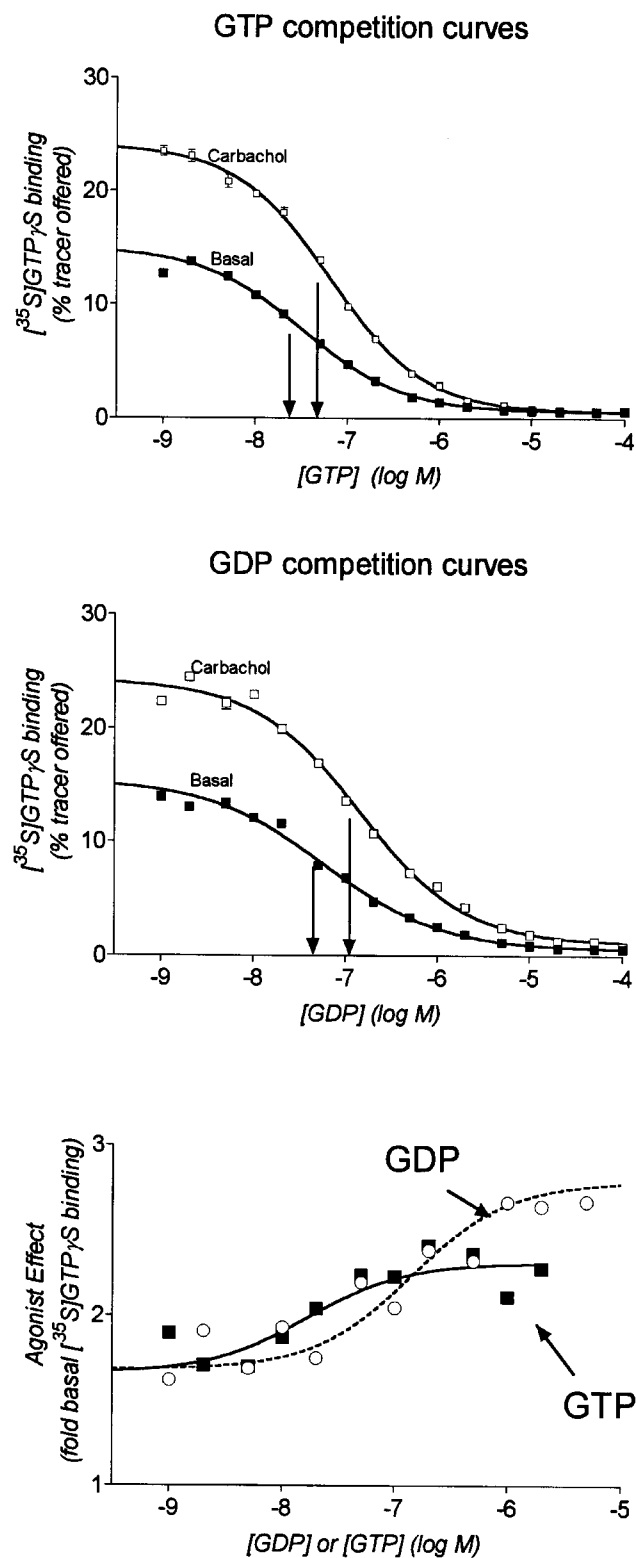


Fig. 6. Effect of agonists on GDP and GTP competition curves. Top and center, [³⁵S]GTP_γS binding was measured in the absence (■) or presence (□) of 1 mM carbamylcholine, in the presence of the indicated concentrations of GTP (top) or GDP (center). The GTP and the GDP pI₅₀ values decreased in the presence of carbamylcholine, from 7.38 ± 0.06 (n_H, 0.65 ± 0.04) to 7.00 ± 0.04 (n_H, 0.82 ± 0.05) and from 7.50 ± 0.03 (n_H, 0.79 ± 0.03) to 7.19 ± 0.03 (n_H, 0.83 ± 0.04), respectively. I calculated in the bottom panel the fold stimulation of [³⁵S]GTP_γS binding by 1 mM carbamylcholine, in the presence of the indicated GDP (○) or GTP (■) concentrations. Representative of three duplicate experiments.

proved in the presence of micromolar concentrations of either nucleotide (Fig. 6, bottom), GDP being less potent but more efficient in this respect than GTP.

The observation that GTP competition curves were shifted to higher concentrations whereas GTPγS competition curves shifted to lower concentrations indicated that the ability of G proteins to hydrolyze GTP but not GTPγS played an important role in this experiment. Biphasic GDP and GTP competition curves could be readily explained under the assumption that GPCRs recognized GDP-bound G proteins (at high GDP or GTP concentrations) faster than empty G proteins; this was partial compensation for the competition between [³⁵S]GTPγS and the unlabeled nucleotide for RG recognition (Appendix). Muscarinic agonists are known to facilitate the release of GDP from the HRG_{GDP} complex; they further accelerated [³⁵S]GTPγS binding to GDP-bound G proteins, by facilitating the ternary complex (HRG) formation from HRG_{GDP}. They therefore facilitated [³⁵S]GTPγS binding in the presence of either GDP or GTP.

Discussion

I investigated the guanyl nucleotide binding properties of CHO cells membranes transfected with M₁ muscarinic receptors in the absence and presence of acetylcholine or carbamylcholine. My GTPγS binding results could not be interpreted using "traditional" binding models: 1) It was impossible to simultaneously fit the [³⁵S]GTPγS association and dissociation kinetics with bimolecular association models (compare Fig. 1 with the top and center panels of Fig. 2). 2) G proteins can "know" about agonist binding only by interacting with an agonist-bound receptor. At very low receptor densities, each receptor nevertheless accelerated GTPγS binding to more than one G protein (Fig. 4).

I developed in the Appendix the equations that describe the catalysis of the reversible G protein-GTPγS binding reaction (Fig. 7). In view of the complexity of the equations as well as the experimental system (multiple G proteins), I did not attempt to obtain quantitative estimates of the six to eight rate constants but merely verified that the predictions of the catalytic model were compatible with my experimental data. I shall hereafter justify the model analyzed, explain intuitively how my experimental results can be explained within a single coherent framework, and point out the implications of the model in the experimental results' interpretation; a formal (mathematical) discussion will be found in the Appendix.

Some experiments were performed in the absence of unlabeled nucleotides. GDP dissociation is slow but not impossible: my results (Table 1) suggested that GPCRs encountered empty G proteins under these incubation conditions (reaction g in Fig. 7b). Other experiments were performed in the presence of high GDP or GTP concentrations. GTP is hydrolyzed by the G protein and the resulting GDP dissociates very slowly from resting G proteins: GPCRs encountered GDP-bound G proteins under these conditions (Fig. 7a, reaction 1). Muscarinic receptors facilitate the GDP release (Fig. 7a, reaction 2) (Berstein et al., 1992), thereby allowing GTPγS binding.

In the absence of GDP or GTP, pertussis toxin pretreatment (that inactivates G_{i/o} proteins) did not affect the basal and agonist-induced [³⁵S]GTPγS binding rate (not shown). The over-basal [³⁵S]GTPγS association rate, in contrast, de-

creased with decreasing receptor concentrations (Table 2). These two results suggested that, even in the absence of agonists, [³⁵S]GTPγS recognized RG complexes rather than uncoupled G proteins (Fig. 7, reaction 3).

After 4-DAMP mustard treatment, the over-basal GTPγS B_{\max} was larger than the muscarinic receptor density (Fig. 4 and Table 2). This implies that GTPγS recognition was followed by the release of the newly formed $G_{GTP\gamma S}^*$ complex (Fig. 7, reaction 4), then by another G protein activation cycle. This model explained in addition the markedly biphasic [³⁵S]GTPγS dissociation kinetics (Fig. 1): two labeled $G_{GTP\gamma S}^*$ populations, $HRG_{GTP\gamma S}^*$ and $G_{GTP\gamma S}^*$, coexisted after GTPγS binding.

The reactions shown in Fig. 7 are cyclic: GTPγS binding cannot proceed faster than the slowest step in the cycle, known as the "rate limiting step". Agonists need to facilitate only this step to accelerate GTPγS binding. It is possible to switch the rate limiting step from RG_e formation (steps g or

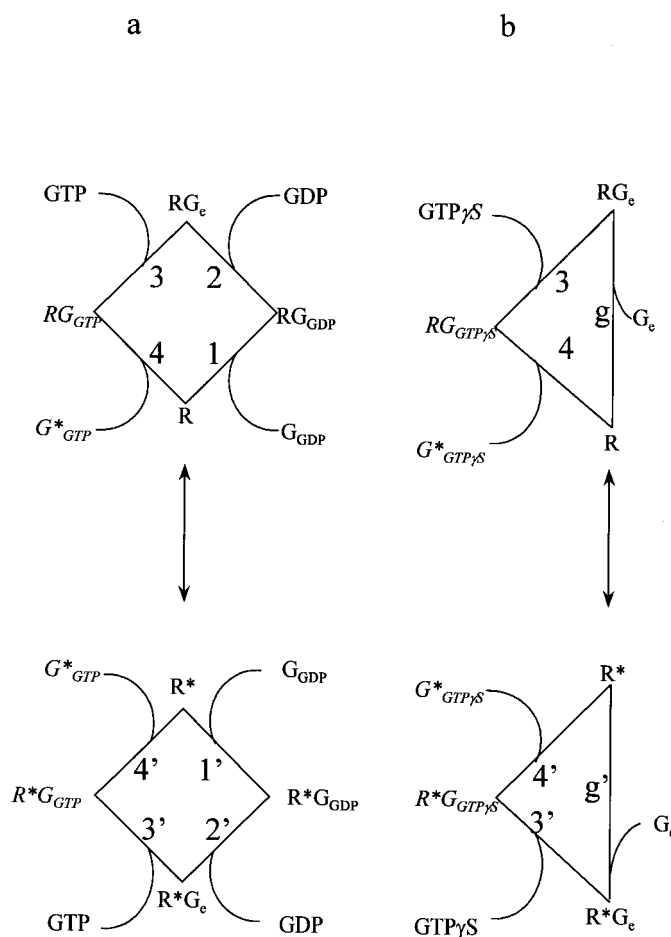


Fig. 7. [³⁵S]GTPγS binding models examined in this work. I assumed in the Appendix and in my previous work (Waelbroeck et al., 1997) that the receptor can be found in two conformations with very low (R) and high (R*) biological activities. I also assumed that the conformational change is rapid when the receptors are uncoupled (R and R* are in equilibrium), but prevented by the receptor-G protein interaction. In GDP- or GTP-containing media (a), the receptors encounter GDP-bound G proteins (reactions 1, 1') and facilitate the GDP release (reactions 2, 2'). The emptied, receptor coupled G protein then recognizes GTPγS or GTP (reactions 3, 3') and the $G_{GTP\gamma S}^*$ complex dissociates from the receptor (reactions 4, 4'). In the absence of other nucleotides (b), the receptors recognize empty G proteins (reactions g, g'). GTPγS recognition by receptor-coupled G proteins (reactions 3, 3') is followed by the $G_{GTP\gamma S}^*$ dissociation (reactions 4, 4').

1–2 in Fig. 7) to GTP γ S recognition (steps 3–4 in Fig. 7) by modifying the incubation conditions, and thereby obtain detailed information about the agonists' activities.

GTP γ S binding (reactions 3–4) is rate limiting at very low tracer concentrations (if [GTP γ S] is small, its association rate, $k_{on}[RG_e][GTP\gamma S]$, is low). [^{35}S]GTP γ S binding was facilitated by M₁ muscarinic agonists in the absence of GDP. GTP γ S inhibited agonists binding at equilibrium: the $HRG_{GTP\gamma S}^*$ complex is unstable. Muscarinic M₁ agonists probably increased the probability of releasing bound $G_{GTP\gamma S}^*$ rather than free [^{35}S]GTP γ S from the intermediate complex, $HRG_{GTP\gamma S}^*$. They recognized G protein-coupled receptors (RG) with a high affinity and were therefore potent at very low nucleotide concentrations (Table 3 and Fig. 5). (Please note that agonist-bound GPCRs usually accelerate little if at all [^{35}S]GTP γ S binding in the absence of GDP (Weiland and Jakobs, 1994); as a rule, they do not accelerate the $G_{GTP\gamma S}^*$ dissociation from $HRG_{GTP\gamma S}^*$.)

In the presence of GTP, most G proteins were occupied by GDP, synthesized in situ by the G protein (Hamm, 1998). Muscarinic M₁ agonists facilitate the release of GDP from their receptor's cognate G proteins (Berstein et al., 1992); they thereby increased the (empty) G protein concentration available for GTP γ S as well as for GTP recognition and therefore accelerated [^{35}S]GTP γ S (and GTP) binding. Agonists also accelerated the activated G protein release, thereby facilitating GTP γ S and GTP binding. GTP, however, competed with [^{35}S]GTP γ S for empty G protein recognition; facilitating the $G_{GTP\gamma S}^*$ release is not sufficient to increase [^{35}S]GTP γ S binding in the presence of GTP. Muscarinic agonists had a low affinity and potency in the presence of GTP.

At high GDP concentrations, most G proteins are GDP-bound. M₁ muscarinic agonists not only facilitated the GDP release from HRG_{GDP} (reaction 2) but also increased the probability of dissociating $G_{GTP\gamma S}^*$ rather than GTP γ S from $HRG_{GTP\gamma S}^*$ (reaction 4). Both effects facilitated synergically [^{35}S]GTP γ S binding: the effect of agonists on [^{35}S]GTP γ S binding was more impressive in the presence of GDP than in the absence or presence of GTP (Fig. 6). Agonists had a low affinity in the presence of GDP (not shown); this explains their low potency (Table 3 and Fig. 5).

GDP and GTP competition curves may deviate from "one site" competition curves even if a single G protein subtype exists, because GPCRs encounter two (empty and GDP-bound) G protein states (see Fig. 8). If agonist-bound receptors activate G_{GDP} more readily than G_e , they will catalyze [^{35}S]GTP γ S binding to GDP-bound G proteins more efficiently in the presence of GDP or GTP, and the competition curves will be shallow. Agonists that facilitate the GDP release further decrease the inhibitory effect of GDP and GTP on [^{35}S]GTP γ S binding and therefore shift the competition curve to higher concentrations (Fig. 6).

Catalysts cannot affect the equilibrium constant of the reactions they accelerate: the $G + GTP\gamma S \leftrightarrow G_{GTP\gamma S}^*$ reaction must have the same equilibrium constant K as the $G + GTP\gamma S + \{R \leftrightarrow RG + GTP\gamma S \leftrightarrow RG_{GTP\gamma S}^* \leftrightarrow R\} + G_{GTP\gamma S}^*$ reaction. If [G], [GTP γ S], and [$G_{GTP\gamma S}^*$] are rate-limiting: the spontaneous and receptor-catalyzed reaction rates can be described by similar equations: $d[G_{GTP\gamma S}^*] / d(t) = k_{on}[G][GTP\gamma S] - k_{off}[G_{GTP\gamma S}^*]$. In the case of bimolecular reversible binding reactions, k_{on} and k_{off} represent the association and dissociation rate constants, respectively; if the reaction

is catalyzed, k_{on} and k_{off} measure the forward and reverse V_{max}/K_m ratios, where V_{max} is the maximum reaction rate and K_m is the substrate or product concentration that supports a half-maximal reaction rate.

By definition, $d[G_{GTP\gamma S}^*] / d(t) = 0$ at equilibrium; because $K = [G_{GTP\gamma S}^*] / [G][GTP\gamma S] = k_{on} / k_{off}$, agonists that increase k_{on} at vanishingly low [G] and [GTP γ S] must necessarily increase k_{off} at vanishingly low [$G_{GTP\gamma S}^*$]. Muscarinic agonists accelerated [^{35}S]GTP γ S binding at rate limiting [RG] and [GTP γ S] by increasing k_{on} , the forward reaction V_{max}/K_m ratio. It is therefore a thermodynamic necessity that they increase k_{off} the [^{35}S]GTP γ S dissociation rate at very low $G_{GTP\gamma S}^*$ concentrations.

In contrast with muscarinic M₂ (Hilf and Jakobs, 1992), fMet-Leu-Phe (Kupprion et al., 1993), or opiate (Breivogel et al., 1998) agonists, muscarinic M₁ agonists did not accelerate the [^{35}S]GTP γ S dissociation (Fig. 1). This suggests that the $G_{GTP\gamma S}^*$ concentration was not rate-limiting but saturating in my experiment. There, results showed that the slow dissociation phase corresponded to the maximal receptor-catalyzed $G_{GTP\gamma S}^*$ dissociation rate, the "reverse V_{max} ".

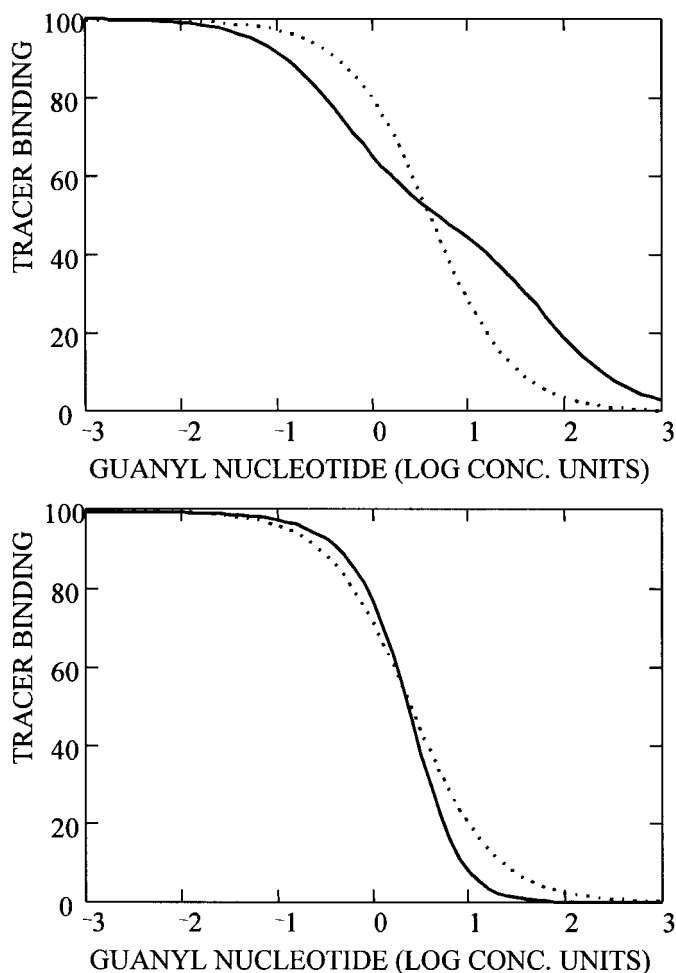


Fig. 8. Biphasic and cooperative competition curves, predicted by the catalytic model of GTP γ S binding. As explained in the Appendix, if the GPCRs catalyze [^{35}S]GTP γ S binding to a single G protein subtype GDP, GTP competition curves may appear biphasic (full line, top) or cooperative (full line, bottom) depending on the rate constants. [A noncooperative competition curve (dotted line) is shown on each panel for comparison.] The GDP dissociation constant from uncoupled G proteins and all the rate constants except the GDP and $G_{GTP\gamma S}^*$ dissociation rates were set to 1; top, [G] = 1, k_2 = 10, k_4 = 30; bottom, [G] = 0.1, k_2 = 0.003, k_4 = 0.3.

Agonists must increase the reverse V_{\max}/K_m ratio but did not affect the reverse V_{\max} ; this means that they decreased the $G_{\text{GTP}\gamma\text{S}}^* K_m$ value (i.e., they increased the receptor- $G_{\text{GTP}\gamma\text{S}}^*$ interaction at steady state). K_m is not equivalent to a dissociation constant: agonists may decrease the $G_{\text{GTP}\gamma\text{S}}^* K_m$ value without affecting its affinity for the receptors by accelerating the $G_{\text{GTP}\gamma\text{S}}^*$ recognition and dissociation to the same extent. To achieve this, agonists perhaps improved the receptor-coupled G proteins' likeness to GTP-bound G proteins: part of the free energy needed to allow reaction 4 is used to change the G protein conformation during the $G_{\text{GTP}\gamma\text{S}}^*$ recognition and dissociation.

I show in Fig. 2, bottom, that tracer binding kinetics comparable with my experimental results (Fig. 1) can indeed be explained by the catalytic model of GTP γ S binding, provided that $G_{\text{GTP}\gamma\text{S}}^*$ has a high affinity for the receptors and competes efficiently with G_e and G_{GDP} for receptor recognition. This interpretation is fully compatible with the observations of Biddlecome et al. (1996), suggesting that the phospholipase C is activated in part by M_1 receptor-coupled, GTP-bound G proteins. It also explains why I observed activation of several G proteins by a single receptor at low but not high receptor concentrations (Table 2 and Fig. 4): [³⁵S]GTP γ S binding was faster at high receptor concentrations, and the $G_{\text{GTP}\gamma\text{S}}^*$ concentration became saturating (and prevented the recognition of empty G proteins) more rapidly at high rather than at low receptor concentrations.

In conclusion, the effect of agonist-activated M_1 muscarinic receptors on [³⁵S]GTP γ S association and dissociation kinetics could not be explained by a bimolecular GTP γ S/G protein binding model. I was able, in contrast, to explain all my experimental results under the assumption that GPCRs catalyzed the nucleotide-G protein interaction in the absence and presence of agonists. My results suggested that M_1 muscarinic receptors efficiently catalyzed GTP γ S binding and that the $G_{\text{GTP}\gamma\text{S}}^*$ complex behaved as a very efficient automatic brake for this "one way" reaction.

References

- Berrie CP, Birdsall NJ, Hulme EC, Keen M and Stockton JM (1984) Solubilization and characterization of guanine nucleotide-sensitive muscarinic agonist binding sites from rat myocardium. *Br J Pharmacol* **82**:853–861.
- Berstein G, Blank JL, Smrcka AV, Higashijima T, Sternweis PC, Exton JH and Ross EM (1992) Reconstitution of agonist-stimulated phosphatidylinositol 4,5-bisphosphate hydrolysis using purified M_1 muscarinic receptor, $G_{q/11}$, and phospholipase C- β_1 . *J Biol Chem* **267**:8081–8088.
- Biddlecome GH, Bernstein G and Ross EM (1996) Regulation of phospholipase C- β_1 by G_q and M_1 muscarinic cholinergic receptor. Steady-state balance of receptor-mediated activation and GTPase-activating protein-promoted deactivation. *J Biol Chem* **271**:7999–8007.
- Birdsall NJ, Burgen AS and Hulme EC (1978) The binding of agonists to brain muscarinic receptors. *Mol Pharmacol* **14**:723–736.
- Birnbaumer L and Birnbaumer M (1995) Signal transduction by G proteins: 1994 Edition. *J Recept Signal Transduct Res* **15**:213–252.
- Breivogel CS, Selley DE and Childers SR (1998) Cannabinoid receptor agonist efficacy for stimulating [³⁵S]GTP γ S binding to rat cerebellar membranes correlates with agonist-induced decreases in GDP affinity. *J Biol Chem* **273**:16865–16873.
- Cassel D and Selinger Z (1978) Mechanism of adenylate cyclase activation through the β -adrenergic receptor: Catecholamine-induced displacement of bound GDP by GTP. *Proc Natl Acad Sci USA* **75**:4155–4159.
- Cheng Y and Prusoff WH (1973) Relationship between the inhibition constant (K_i) and the concentration of inhibitor which causes 50 per cent inhibition (I_{50}) of an enzymatic reaction. *Biochem Pharmacol* **22**:3099–3108.
- Chidiac P, Markin VS and Ross EM (1999) Kinetic control of guanine nucleotide binding to soluble $G_{\alpha(q)}$. *Biochem Pharmacol* **58**:39–48.
- Cornish-Bowden A (1995) *Fundamentals of Enzyme Kinetics*, Portland Press, London.
- Costa T, Ogino Y, Munson PJ, Onaran HO and Rodbard D (1992) Drug efficacy at guanine nucleotide-binding regulatory protein-linked receptors: Thermodynamic interpretation of negative antagonism and of receptor activity in the absence of ligand. *Mol Pharmacol* **41**:549–560.
- De Lean A, Stadel JM and Lefkowitz RJ (1980) A ternary complex model explains the agonist-specific binding properties of the adenylate cyclase-coupled β -adrenergic receptor. *J Biol Chem* **255**:7108–7117.
- Ferguson KM, Higashijima T, Smigel MD and Gilman AG (1986) The influence of bound GDP on the kinetics of guanine nucleotide binding to G Proteins. *J Biol Chem* **261**:7393–7399.
- Florio VA and Sternweis PC (1985) Reconstitution of resolved muscarinic cholinergic receptors with purified GTP-binding proteins. *J Biol Chem* **260**:3477–3483.
- Haga K, Haga T and Ichiyama A (1986) Reconstitution of the muscarinic acetylcholine receptor. Guanine nucleotide-sensitive high affinity binding of agonists to purified muscarinic receptors reconstituted with GTP-binding proteins (G_i and G_o). *J Biol Chem* **261**:10133–10140.
- Haga K, Haga T, Ichiyama A, Katada T, Kurose H and Ui M (1985) Functional reconstitution of purified muscarinic receptors and inhibitory guanine nucleotide regulatory protein. *Nature (Lond)* **316**:731–733.
- Hamm HE (1998) The many faces of G protein signaling. *J Biol Chem* **273**:669–672.
- Hilf G and Jakobs KH (1992) Activation of solubilized G-proteins by muscarinic acetylcholine receptors. *Cell Signal* **4**:787–794.
- Hulme EC, Berrie CP, Birdsall NJ and Burgen AS (1981) Two populations of binding sites for muscarinic antagonists in the rat heart. *Eur J Pharmacol* **73**:137–142.
- Krumins AM, Lapeyre JN, Clark RB and Barber R (1997) Evidence for the shuttle model for G_{α} activation of adenyl cyclase. *Biochem Pharmacol* **54**:43–59.
- Kupprion C, Wieland T and Jakobs KH (1993) Receptor-stimulated dissociation of GTP γ [S] from G_i -proteins in membranes of HL-60 cells. *Cell Signal* **5**:425–433.
- Lazareno S, Farries T and Birdsall NJ (1993) Pharmacological characterization of guanine nucleotide exchange reactions in membranes from CHO cells stably transfected with human muscarinic receptors M_1 - M_4 . *Life Sci* **52**:449–456.
- Mackay D (1990) Interpretation of relative potencies, relative efficacies and apparent affinity constants of agonist drugs estimated from concentration-response curves. *J Theor Biol* **142**:415–427.
- Motulsky HJ and Mahan LC (1984) The kinetics of competitive radioligand binding predicted by the law of mass action. *Mol Pharmacol* **25**:1–9.
- Mukhopadhyay S and Ross EM (1999) Rapid GTP binding and hydrolysis by $G_{(q)}$ promoted by receptor and GTPase-activating proteins. *Proc Natl Acad Sci USA* **96**:9539–9544.
- Onaran HO, Costa T and Rodbard D (1993) $\beta\gamma$ subunits of guanine nucleotide-binding proteins and regulation of spontaneous receptor activity: Thermodynamic model for the interaction between receptors and guanine nucleotide-binding protein subunits. *Mol Pharmacol* **43**:245–256.
- Waelbroeck M (1999) Kinetics versus equilibrium: The importance of GTP in GPCR activation. *Trends Pharmacol Sci* **20**:477–481.
- Waelbroeck M (2001) Activation of guanosine 5'-[γ -³⁵S]thio-triphosphate binding through M_1 muscarinic receptors in transfected Chinese hamster ovary cell membranes: 2. Testing the "two-states" model of receptor activation. *Mol Pharmacol* **59**:886–893.
- Waelbroeck M, Boufrah L and Swillens S (1997) Seven helix receptors are enzymes catalysing G protein activation. What is the agonist K_{act} ? *J Theor Biol* **187**:15–37.
- Waelbroeck M, Camus J and Christophe J (1989) Determination of the association and dissociation rate constants of muscarinic antagonists on rat pancreas: Rank order of potency varies with time. *Mol Pharmacol* **36**:405–411.
- Waelbroeck M, Robberecht P, Chatelain P and Christophe J (1982) Rat cardiac muscarinic receptors. I. effects of guanine nucleotides on high- and low-affinity binding sites. *Mol Pharmacol* **21**:581–588.
- Weiland T and Jakobs KH (1994) Measurement of receptor-stimulated guanosine 5'-O-(γ -Thio)triphosphate binding by G proteins. *Methods Enzymol* **237**:3–13.

Send reprint requests to: Dr. Waelbroeck, Laboratoire de Chimie Biologique et de la Nutrition, Faculté de Médecine de l'Université Libre de Bruxelles, Bât. G/E, CP 611, 808 Route de Lennik, B-1070 Brussels, Belgium. E-mail: mawaelbr@ulb.ac.be